



Inhibiting HIF-1 α by 2ME2 ameliorates early brain injury after experimental subarachnoid hemorrhage in rats



Cheng Wu¹, Qiang Hu¹, Jingyin Chen, Feng Yan, Jianru Li, Lin Wang, Hangbo Mo, Chi Gu, Peng Zhang, Gao Chen^{*}

Department of Neurosurgery, The Second Affiliated Hospital of Zhejiang University School of Medicine, No. 88 Jiefang road, Hangzhou 310009, China

ARTICLE INFO

Article history:

Received 20 June 2013

Available online 9 July 2013

Keywords:

Subarachnoid hemorrhage
Hypoxia-inducible factor-1 α
Early brain injury
2ME2
VEGF
BNIP3

ABSTRACT

Although hypoxia-inducible factor-1 α (HIF-1 α) has been extensively studied in brain injury following hypoxia–ischemia, the role of HIF-1 α in early brain injury (EBI) after subarachnoid hemorrhage (SAH) remains unclear. The present study was undertaken to investigate a potential role of HIF-1 α in EBI after SAH. Rats ($n = 60$) were randomly divided into sham+vehicle, SAH+2-methoxyestradiol (2ME2), and SAH+vehicle groups. The SAH model was induced by endovascular perforation and all the rats were subsequently sacrificed at 24 h after SAH. We found that treatment with 2ME2 suppressed the expression of HIF-1 α , BNIP3 and VEGF and reduced cell apoptosis, blood–brain barrier (BBB) permeability, brain edema, and neurologic scores. Double fluorescence labeling revealed that HIF-1 α was expressed predominantly in the nuclei of neurons and TUNEL-positive cells. Our work demonstrated that HIF-1 α may play a role in EBI after SAH, causing cell apoptosis, BBB disruption, and brain edema by up-regulating its downstream targets, BNIP3 and VEGF. These effects were blocked by the HIF-1 α inhibitor, 2ME2.

© 2013 Elsevier Inc. All rights reserved.

1. Introduction

Aneurysmal subarachnoid hemorrhage (SAH) is a devastating disease with high morbidity and mortality, with up to 50% of SAH survivors experiencing persistent neurological deficits [1]. Early brain injury (EBI) after SAH is considered a major underlying cause of the poor outcomes for SAH patients [2,3]. EBI refers to the immediate cerebral injury that occurs within 72 h after SAH, including brain cell death, blood–brain barrier (BBB) disruption, brain edema, and the dysfunction of microvasculature [4]. It has been revealed that cerebral ischemia, resulting from sudden intracranial pressure elevation and global cerebral blood flow reduction, might play an important role in EBI after SAH [5]. However, the molecular mechanisms of EBI after SAH remain poorly understood.

Hypoxia-inducible factor-1 (HIF-1), composed of the hypoxia-regulated subunit HIF-1 α and the oxygen-insensitive subunit HIF-1 β , is a key endogenous signaling protein triggered by ischemia or hypoxia [6]. In particular, HIF-1 α is up-regulated by hypoxia and modulates the expression of multiple genes to initiate various physiological responses against hypoxic conditions [7]. HIF-1 α has also been reported to accumulate in brains exposed to SAH, though its potential role in EBI after SAH remains controversial [8–11]. HIF-1 α has many roles in the cell. It serves as a pro-apoptotic factor

by stabilizing the p53 tumor suppressor protein [12] and by up-regulating BNIP3 (BCL2/adenovirusE1B 19 kDa interacting protein 3), a pro-apoptotic protein containing the BH3 domain [7,13,14]. Of particular note, HIF-1 α also enhances the permeability of the BBB by stimulating vascular endothelial growth factor (VEGF) [15]. In addition, it has been shown that neuron apoptosis and vasculature subjected to SAH-induced cerebral ischemia are key to EBI after SAH; EBI often involves disruption of the BBB and development of brain edema [16]. However, it is unclear whether HIF-1 α contributes to cell apoptosis, dysfunction of the BBB and the subsequent brain edema by up-regulating BNIP3 and VEGF.

Therefore, the current study was designed to investigate whether acute inhibition of HIF-1 α by 2-methoxyestradiol (2ME2), a HIF-1 α inhibitor, provides neuroprotection against EBI after SAH by preventing the stimulation of BNIP3 and VEGF in a rat model of SAH using endovascular perforation.

2. Materials and methods

2.1. Animals

Male Sprague–Dawley Rats (280–320 g) obtained from the SLAC Laboratory Animal Co. Ltd (Shanghai, China) were fed on standard pellet chow and water *ad libitum* (22 \pm 2 $^{\circ}$ C, a 12 h light/dark cycle). All experimental procedures were approved by the Ethics Committee for the Use of Experimental Animals. Sixty rats were randomly assigned into three groups: sham+vehicle group

^{*} Corresponding author. Fax: +86 057187784753.

E-mail address: d.chengao@163.com (G. Chen).

¹ These authors contributed equally to this work.

($n = 20$), subjected to the SAH procedure but without perforation, received DMSO as the vehicle; SAH+2ME2 group ($n = 20$), subjected to SAH and treated with 2ME2; SAH+vehicle group ($n = 20$), subjected to SAH and treated with the same volume of vehicle as the sham+vehicle group. All rat brain samples were extracted 24 h after surgery.

2.2. The rat SAH model

The rat SAH model was induced by endovascular perforation as in a previous study, with slight modifications [3]. Briefly, rats were anesthetized with 1% sodium pentobarbital (40 mg/kg, i.p.), and the right external carotid artery (ECA) was isolated and severed, leaving a stump. The internal carotid artery (ICA) and the common carotid artery (CCA) were clamped with vascular clips. The stump of the ECA was reopened, and a blunted 3–0 monofilament nylon suture was inserted up through the ICA until resistance was felt (18–20 mm from the common carotid bifurcation). The suture was carefully pushed approximately 3 mm further to perforate the artery wall. Sham-operated rats underwent an identical procedure without perforation.

2.3. Drug administration

The inhibitor of HIF-1 α , 2-Methoxyestradiol (2ME2, Sigma–Aldrich Corp), was dissolved in dimethyl sulfoxide (DMSO) and further diluted in phosphate buffered saline (PBS) to a final volume of 2 ml. The inhibitor was administered (5 mg/kg, i.p.) 1 h after SAH. The rats in the sham+vehicle group and SAH+vehicle group were injected with same volume of DMSO diluted in PBS.

2.4. Mortality, neurologic score and SAH severity evaluation

Neurologic score was evaluated by an observer blind to the treatment group at 24 h after SAH, based on the scoring system reported by Garcia [17] with slight modifications. Mortality was calculated at the same time. The severity of SAH was quantified by the grading scale of Sugawara [18], with modifications.

2.5. Measurement of brain water content

Rats ($n = 5$) were sacrificed under deep anesthesia 1% sodium pentobarbital (60 mg/kg, i.p.) after 24 h of SAH. The brains were rapidly removed and weighed immediately (wet weight). Brains were then dried in an oven at 105 °C for 24 h and weighed again (dry weight). Brain water content was calculated as [(wet weight–dry weight)/wet weight] \times 100%.

2.6. Determination of BBB permeability

BBB permeability was quantitatively evaluated by Evans blue (EB) extravasation at 24 h after SAH. Briefly, rats ($n = 5$) were injected intravenously with 2% EB dye (5 ml/kg, Sigma–Aldrich Corp). One hour later, rats were anesthetized with sodium pentobarbital (60 mg/kg, i.p.) and perfused with PBS to remove the intravascular EB dye. The brain was then weighed, homogenized in PBS and centrifuged (15,000g, 30 min, 4 °C). The supernatant (0.7 ml) was added to an equal volume of trichloroacetic acid with ethanol (1:3). The samples were incubated overnight at 4 °C and then centrifuged (15,000g, 30 min, 4 °C). The supernatant was quantified for absorbance of EB dye using a spectrophotometer (excitation 620 nm, emission 680 nm).

2.7. Histology and TUNEL staining assay

Rats ($n = 5$) were deeply anesthetized and sacrificed by intracardial perfusion with PBS and 4% ice-cold paraformaldehyde (pH 7.4). The brain was quickly removed, immersed in 30% sucrose solution for at least 48 h, and then cut into 7 μ m thick coronal sections on a cryostat (Leica CM1950). Apoptotic cell death was detected using a TUNEL staining Kit (POD, Roche Applied Science, USA). Briefly, brain sections were incubated with 3% hydrogen peroxide (10 min), permeabilization solution (2 min), and TUNEL reaction mixture (60 min) at 37 °C. Cell nuclei were stained with DAPI (1 μ g/ml, Roche Applied Science, USA). Cell counting was performed in the ipsilateral basal cortex under a fluorescent microscope (Olympus). The total number of cells (DAPI⁺) and the TUNEL-positive cells were counted in five separate fields in three different slices.

2.8. Double fluorescence labeling

To identify neurons that were both HIF-1 α -positive and TUNEL-positive, double fluorescence labeling was performed on brain sections. The double labeling was conducted according to previously described protocols [19,20]. The primary antibodies used were a rabbit antibody to HIF-1 α (1:200, ab51608, Abcam) and mouse antibodies to neuronal nuclei (NeuN) (1:200, MAB377, Millipore) and glial fibrillary acidic protein (GFAP) (1:200, MAB360, Millipore). The secondary antibodies used were rhodamine-conjugated goat anti-rabbit antibody (1:200, Jackson ImmunoResearch) and fluorescein isothiocyanate-labeled goat anti-mouse antibody (1:200, Jackson ImmunoResearch).

To locate HIF-1 α , TUNEL staining was followed by incubation with PBS containing 10% normal goat serum and 0.25% Triton X-100 to block nonspecific binding. Subsequently, brain sections were incubated with primary antibody against HIF-1 α overnight at 4 °C. The sections then were washed and incubated with secondary antibody for 2 h at room temperature.

2.9. Western blots

Anesthetized rats ($n = 5$) were perfused with 250 ml ice-cold PBS (pH 7.4). Brain samples were removed and preserved at –80 °C. Western blotting was performed as described previously with some modifications [21]. Briefly, a brain sample from the ipsilateral basal cortex was homogenized and then centrifuged (15,000g, 15 min, 4 °C). The protein content was measured with a Bio-Rad protein assay. Equal amounts of protein (60 μ g) were resuspended in loading buffer, denatured at 95 °C for 10 min, and loaded into the wells of sodium dodecyl sulfate–polyacrylamide gels. The samples were electrophoresed at 80 v for 4 h and transferred to polyvinylidene fluoride membranes at 100 v for 2 h. The membrane was blocked with nonfat dry milk buffer and probed overnight at 4 °C with primary rabbit antibodies against HIF-1 α (1:1000, ab51608, Abcam), BNIP3 (1:1000, ab10433, Abcam), VEGF (1:1000, ab46154, Abcam), and β -actin (1:2000, Santa Cruz). Following washes, membranes were incubated with horseradish peroxidase-conjugated secondary antibodies for 1 h at room temperature. The protein band density was detected by X-ray film and quantified using Image J software (NIH).

2.10. Statistical analysis

Data were expressed as mean \pm SD. Statistical significance was analyzed by one-way analysis of variance followed by the Tukey test for multiple comparisons. Mortality was analyzed by a chi square test. A value of $P < 0.05$ was considered statistically significant.

3. Results

3.1. Physiological variables

Body temperature (36.5–37.5 °C), mean arterial pressure (80–120 mmHg), arterial pH (7.35–7.45), PO₂ (80–100 mmHg), PCO₂ (35–45 mmHg) and blood glucose (85–120 mg/dl) were monitored throughout the surgical procedure. All physiological variables were in a normal range, and there were no significant differences among the groups (data not shown).

3.2. Mortality, neurologic scores and SAH grade

Mortality was 35.00% in the SAH+vehicle group and 25.00% in the SAH+2ME2 group with no significant differences ($P > 0.05$, Fig. 1A). No rats in the sham+vehicle group died. Neurologic scores in the SAH+vehicle group and the SAH+2ME2 group were both significantly lower than in the sham+vehicle group ($P < 0.05$, Fig. 1B). However, 2ME2 significantly reduced the neurologic scores compared with the SAH+vehicle group ($P < 0.05$, Fig. 1B). At 24 h after SAH, subarachnoid blood clots were particularly found on the ipsilateral side, around the circle of Willis and ventral brainstem. The SAH grading scores in the sham+vehicle group, SAH+vehicle group and SAH+2ME2 group were 0 ± 0 , 13.65 ± 2.01 and 13.45 ± 1.82 , respectively. Treatment with 2ME2 did not alter the grade of SAH compared to that of the SAH+vehicle group ($P > 0.05$, Fig. 1C).

3.3. Effect of 2ME2 on brain water content

The brain water content in the sham+vehicle group was $79.12 \pm 0.10\%$ (Fig. 1D). A significant increase in water content was observed in the brain samples at 24 h after SAH when compared with animals in the sham+vehicle group ($P < 0.05$). 2ME2 markedly reduced brain water content ($79.39 \pm 0.15\%$) compared to the SAH+vehicle group ($79.79 \pm 0.24\%$, $P < 0.05$, Fig. 1D).

3.4. Effect of 2ME2 on BBB permeability

At 24 h after SAH, a significant extravasation of EB, an index of BBB disruption, was found in the SAH+vehicle group compared to the sham+vehicle group ($P < 0.05$, Fig. 1E). Treatment with 2ME2 significantly decreased EB extravasation compared with the SAH+vehicle group ($P < 0.05$, Fig. 1E).

3.5. Effect of 2ME2 on cell apoptosis

Few TUNEL-positive cells were found in the ipsilateral basal cortex in the sham+vehicle group at 24 h after SAH, while an increased number of TUNEL-positive cells were detected in the SAH+vehicle group ($P < 0.05$). Treatment with 2ME2 significantly reduced the number of TUNEL-positive cells in the ipsilateral basal cortex ($P < 0.05$, Fig. 2). Double fluorescence labeling of HIF-1 α with NeuN, GFAP, and TUNEL revealed that HIF-1 α expression was pronounced in the nuclei of neurons and TUNEL-positive cells. Only a few astrocytes demonstrated HIF-1 α expression (Fig. 3).

3.6. Effect of 2ME2 on HIF-1 α , BNIP3, and VEGF expression

At 24 h after SAH, the expression levels of HIF-1 α and its downstream targets, BNIP3 and VEGF, were significantly up-regulated in the ipsilateral basal cortex in the SAH+vehicle group compared with the sham+vehicle group ($P < 0.05$, Fig. 4). This up-regulation was markedly inhibited by 2ME2 ($P < 0.05$, Fig. 4).

4. Discussion

The main findings of the current study are summarized as follows: (1) Cell apoptosis, BBB disruption and cerebral edema were aggravated by 24 h of SAH with the up-regulation of HIF-1 α , BNIP3 and VEGF in the ipsilateral basal cortex; (2) Double fluorescence labeling revealed that HIF-1 α expression was pronounced in the

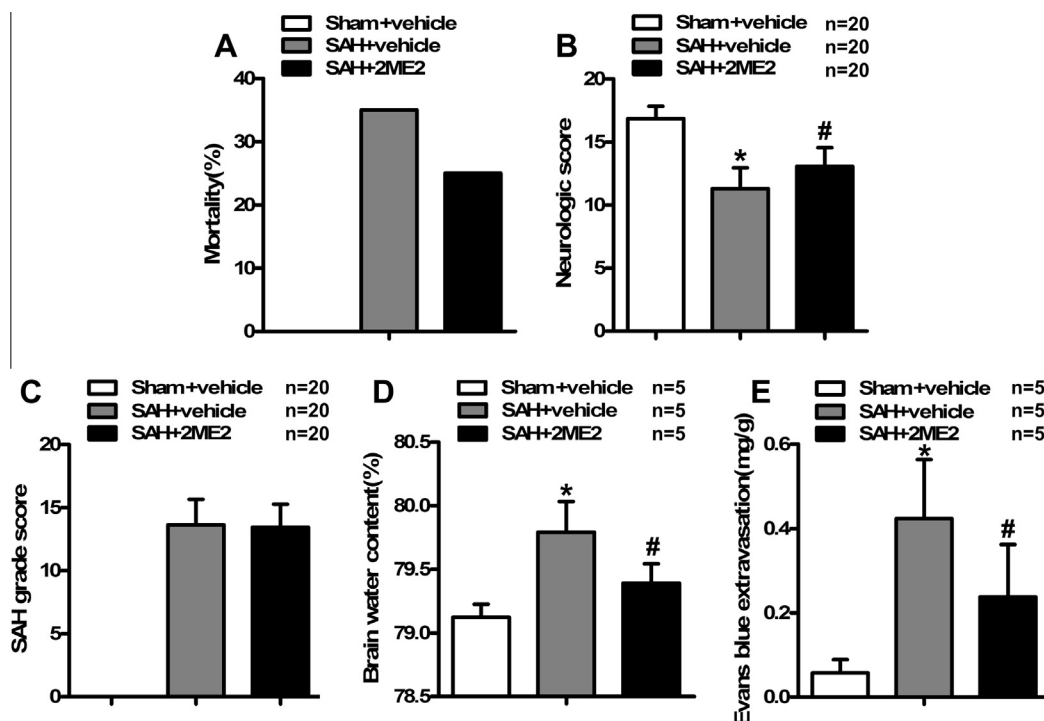


Fig. 1. Effect of 2ME2 on mortality (A), neurological score (B), SAH grade (C), brain water content (D), and Evans blue extravasation (E) in rats 24 h after SAH. Data are shown as mean \pm SD. * $P < 0.05$ vs. sham+vehicle group; # $P < 0.05$ vs. SAH+vehicle group.

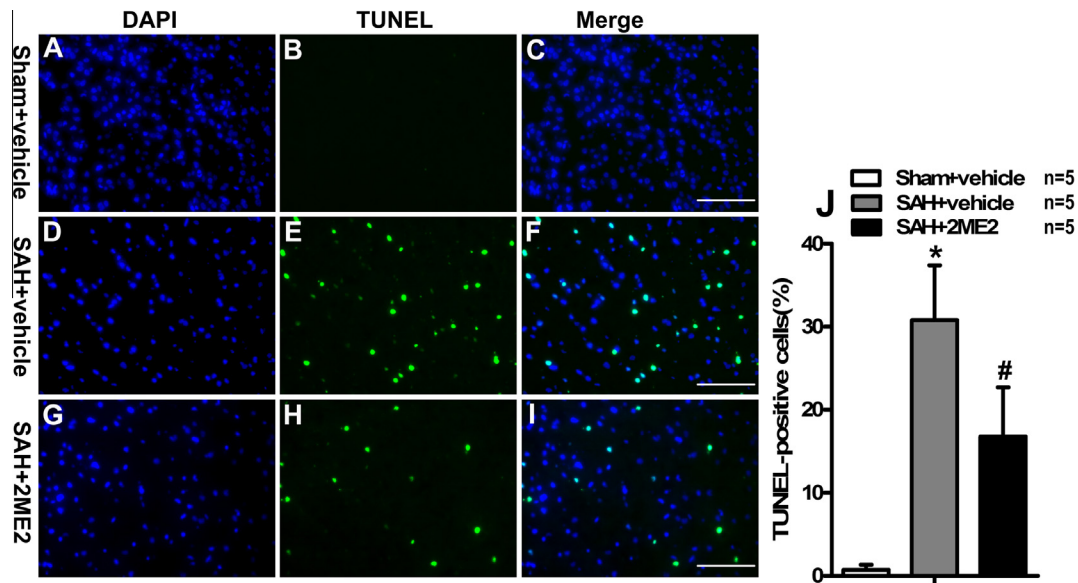


Fig. 2. Effect of 2ME2 on cell apoptosis in the ipsilateral basal cortex at 24 h after SAH. (A–I) Representative TUNEL/DAPI photomicrographs of the ipsilateral basal cortex in different groups. (J) Quantification of TUNEL-positive cells in the groups, expressed as percentage of total (DAPI+) cells. Data are shown as mean \pm SD. * $P < 0.05$ vs. sham+vehicle group; # $P < 0.05$ vs. SAH+vehicle group. Scale bars: 100 μ m.

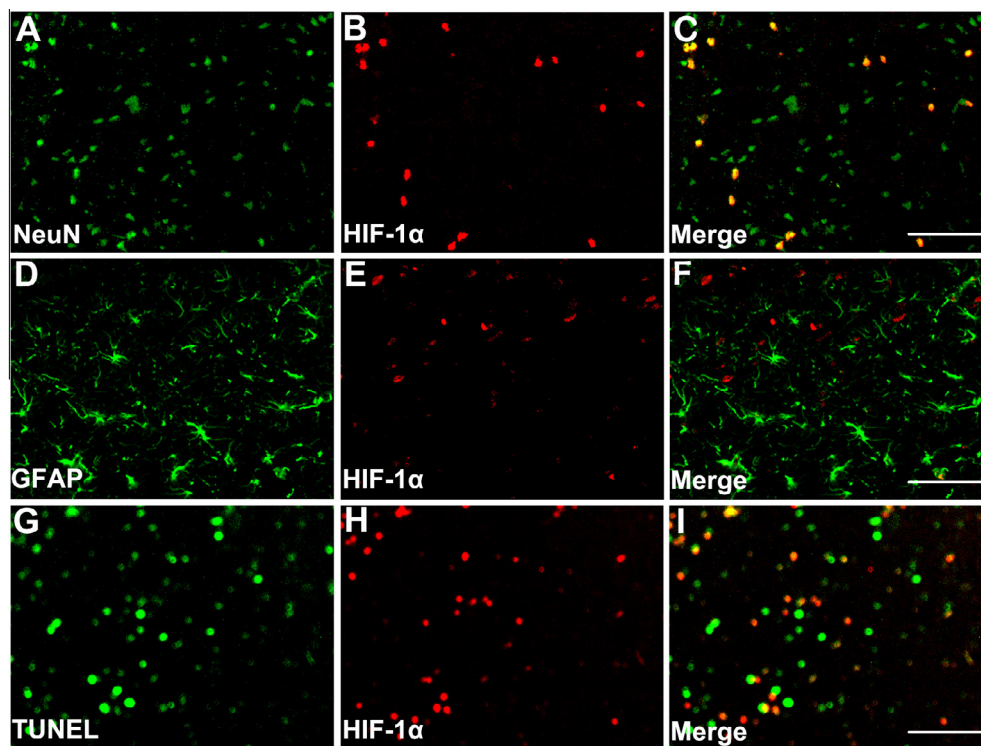


Fig. 3. Double fluorescence labeling of HIF-1 α /NeuN (A–C), HIF-1 α /GFAP (D–F), and HIF-1 α /TUNEL (G–I) in the ipsilateral basal cortex at 24 h after SAH. Scale bars: 100 μ m.

nuclei of neurons and TUNEL-positive cells 24 h after SAH; (3) Treatment with 2ME2 alleviated cerebral injuries and the up-regulation of HIF-1 α , BNIP3 and VEGF induced by SAH. Taken together, these data indicate that activating HIF-1 α and its downstream targets, BNIP3 and VEGF, is crucial in EBI after SAH, and these effects were blocked by 2ME2, a HIF-1 α inhibitor.

Previous studies indicated that HIF-1 α is activated in traumatic brain injury [22], cerebral ischemia [23,24], and cerebral hemorrhage [25]. Both beneficial and detrimental effects of HIF-1 α have

been extensively reported in various models of cerebral ischemia [26–29]. One possible explanation for the discrepancies between these studies is that HIF-1 α may have a dual effect that depends on the severity of the ischemic insult. Although several studies demonstrated that HIF-1 α accumulated following SAH [8–11], the benefit or harm of HIF-1 α elevation is still elusive. Hishikawa et al. [11] revealed that a deferoxamine-induced increase in HIF-1 α protein level and activity significantly attenuated basilar artery vasospasm and reduced brainstem blood flow in a rat model of

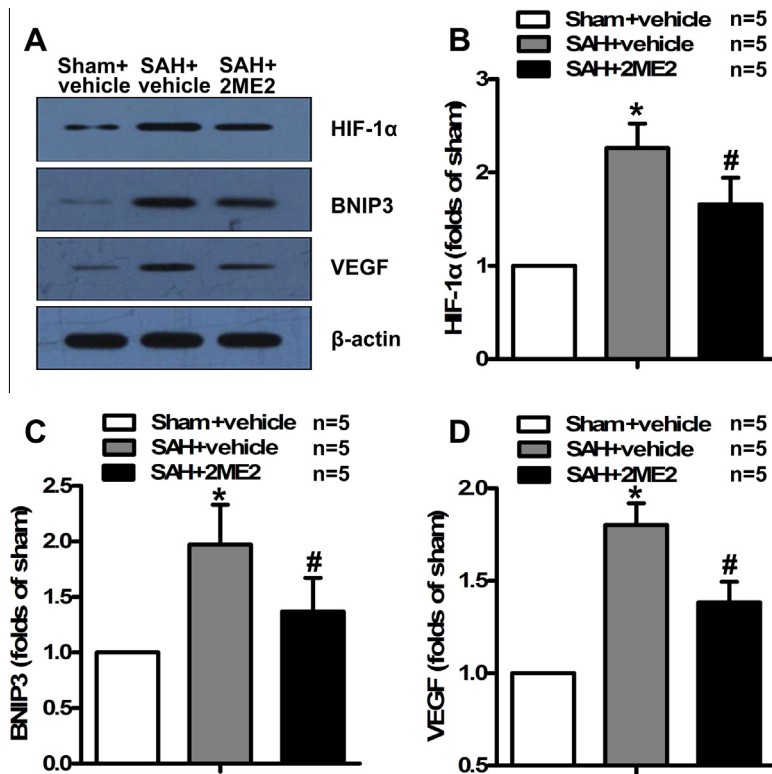


Fig. 4. Effect of 2ME2 on the expression of HIF-1 α (A, B), BNIP3 (A, C), and VEGF (A, D) in the ipsilateral basal cortex at 24 h after SAH. Relative optical densities (O.D.) of HIF-1 α , BNIP3 and VEGF were normalized to β -actin and displayed as the fold-expression over the sham+ group. Data are shown as mean \pm SD. * $P < 0.05$ vs. sham+vehicle group; # $P < 0.05$ vs. SAH+vehicle group.

SAH. In contrast, HIF-1 α stabilization in the basilar artery has been reported to be an important factor in the development of cerebral vasospasm in a rat endovascular perforation model of SAH. Further, 2ME2 was shown to be a powerful agent to attenuate the cerebral vasospasm 48 h after SAH [9]. Ostrowski et al. [8] first reported the expression of HIF-1 α in brain tissue in a rat model of SAH. The researchers speculated that hyperbaric oxygen induced neuroprotection against EBI, partly by inhibition of HIF-1 α and its target proteins. In agreement with previous studies, our study found that a clear up-regulation of HIF-1 α , BNIP3, and VEGF was induced by 24 h of SAH. The protein up-regulation was reversed by the HIF-1 α inhibitor 2ME2, without causing significant changes in intracranial pressure, cerebral perfusion pressure, or cerebral blood flow. These results indicated that 2ME2 reduced EBI after SAH, likely by inhibition of HIF-1 α and downstream targets BNIP3 and VEGF, which led to the decrease in cell apoptosis and preservation of BBB function.

A growing body of evidence suggests that the function of mitochondria is disturbed in the early apoptotic process and may be crucial in mediating apoptosis [30,31]. BNIP3 influences mitochondrial function and can overcome Bcl-2 suppression of apoptosis [32,33]. Previous work by Bruick [34] indicated that BNIP3, activated by HIF-1 α , plays a dedicated role in the progression of hypoxia-mediated apoptosis. It has been reported that BNIP3 is regulated by HIF-1 α and induces apoptotic cell death following focal cerebral ischemia in rats [35,36]. In this study, we showed that HIF-1 α was expressed mainly in the nuclei of neurons and co-localized with TUNEL-positive cells. Further, BNIP3 was up-regulated accompanying HIF-1 α . Taken together, these data suggest HIF-1 α potentially leads to neuron apoptosis by activation of BNIP3 in the ipsilateral basal cortex at 24 h after SAH. The neuroprotective effects of 2ME2 further demonstrate that inhibition of HIF-1 α might be an effective strategy to reduce EBI after SAH.

Early pathological sequelae, such as increased BBB permeability and cerebral edema formation, are common in SAH patients [37]. The up-regulation of VEGF found in brain tissues after SAH may exacerbate BBB disruption [38,39]; in strong support, several studies showed that inhibition of VEGF significantly attenuated brain edema induced by cerebral ischemia/reperfusion [40] and SAH [4]. In addition, suppression of VEGF by a HIF-1 α inhibitor was found to ameliorate BBB breakdown in hypoxic-ischemic brains [28]. However, little is known about the relationship between HIF-1 α and VEGF in rats after SAH. In this study, the decrease in brain water content, BBB permeability and VEGF expression in the SAH+2ME2 group indicates that suppression of VEGF via 2ME2 might be the key to attenuating the BBB disruption induced by SAH. However, besides VEGF, other factors may also contribute to increased BBB permeability after SAH. Recent work by Wang et al. [10] showed that HIF-1 α played a role in cerebral edema formation and BBB disruption via a molecular signaling pathway involving Aquaporin-4 and Matrix Metalloproteinase-9. It is possible that down-regulation of VEGF by acute HIF-1 α inhibition is one of multiple mechanisms that attenuates BBB disruption and brain edema after SAH.

Interestingly, the present study revealed that the mortality of the SAH+2ME2 group (25.00%) was lower than that of the SAH+vehicle group (35.00%), but this difference between the groups was not significant (chi square test, $P > 0.05$). However, a study by Yan et al. [9] showed that 2ME2 significantly reduced mortality after 48 h of SAH in rats. These results indicate that further studies are necessary to explore the dose response and time window of the beneficial effects of 2ME2 in EBI after SAH.

In summary, our current work demonstrated that HIF-1 α may play a role in EBI after SAH, causing cell apoptosis, BBB disruption, and brain edema. When HIF-1 α and its downstream targets, BNIP3

and VEGF, were blocked by HIF-1 α inhibitor 2ME2, EBI was ameliorated.

Acknowledgments

This work was supported by Grants from the National Natural Science Foundation of China (No. 81171094), Grants from the National Science Foundation of Zhejiang province (No. LY13H090001), and a Grant-in-aid for Scientific Research from the Chinese Ministry of Health (No. WKJ2009-2-025).

References

- [1] E.S. Connolly Jr., A.A. Rabinstein, J.R. Carhuapoma, C.P. Derdeyn, J. Dion, R.T. Higashida, B.L. Hoh, C.J. Kirkness, A.M. Naidech, C.S. Ogilvy, A.B. Patel, B.G. Thompson, P. Vespa, Guidelines for the management of aneurysmal subarachnoid hemorrhage: a guideline for healthcare professionals from the American Heart Association/American Stroke Association, *Stroke* 43 (2012) 1711–1737.
- [2] J. Cahill, J.W. Calvert, J.H. Zhang, Mechanisms of early brain injury after subarachnoid hemorrhage, *J. Cereb. Blood Flow Metab.* 26 (2006) 1341–1353.
- [3] J.B. Bederson, I.M. Germano, L. Guarino, Cortical blood flow and cerebral perfusion pressure in a new noncraniotomy model of subarachnoid hemorrhage in the rat, *Stroke* 26 (1995) 1086–1091.
- [4] G. Kusaka, M. Ishikawa, A. Nanda, D.N. Granger, J.H. Zhang, Signaling pathways for early brain injury after subarachnoid hemorrhage, *J. Cereb. Blood Flow Metab.* 24 (2004) 916–925.
- [5] F.A. Sehba, J.B. Bederson, Mechanisms of acute brain injury after subarachnoid hemorrhage, *Neurol. Res.* 28 (2006) 381–398.
- [6] G.L. Wang, B.H. Jiang, E.A. Rue, G.L. Semenza, Hypoxia-inducible factor 1 is a basic-helix-loop-helix-PAS heterodimer regulated by cellular O₂ tension, *Proc. Natl. Acad. Sci. USA* 92 (1995) 5510–5514.
- [7] G.L. Semenza, F. Agani, D. Feldser, N. Iyer, L. Kotch, E. Laughner, A. Yu, Hypoxia, HIF-1, and the pathophysiology of common human diseases, *Adv. Exp. Med. Biol.* 475 (2000) 123–130.
- [8] R.P. Ostrowski, A.R. Colohan, J.H. Zhang, Mechanisms of hyperbaric oxygen-induced neuroprotection in a rat model of subarachnoid hemorrhage, *J. Cereb. Blood Flow Metab.* 25 (2005) 554–571.
- [9] J. Yan, C. Chen, J. Lei, L. Yang, K. Wang, J. Liu, C. Zhou, 2-methoxyestradiol reduces cerebral vasospasm after 48 h of experimental subarachnoid hemorrhage in rats, *Exp. Neurol.* 202 (2006) 348–356.
- [10] Z. Wang, C.J. Meng, X.M. Shen, Z. Shu, C. Ma, G.Q. Zhu, H.X. Liu, W.C. He, X.B. Sun, L. Huo, J. Zhang, G. Chen, Potential contribution of hypoxia-inducible factor-1 α , aquaporin-4, and matrix metalloproteinase-9 to blood–brain barrier disruption and brain edema after experimental subarachnoid hemorrhage, *J. Mol. Neurosci.* 48 (2012) 273–280.
- [11] T. Hishikawa, S. Ono, T. Ogawa, K. Tokunaga, K. Sugiu, I. Date, Effects of deferoxamine-activated hypoxia-inducible factor-1 on the brainstem after subarachnoid hemorrhage in rats, *Neurosurgery* 62 (2008) 232–240.
- [12] W.G. An, M. Kanekal, M.C. Simon, E. Maltepe, M.V. Blagosklonny, L.M. Neckers, Stabilization of wild-type p53 by hypoxia-inducible factor 1 α , *Nature* 392 (1998) 405–408.
- [13] R. Schmidt-Kastner, C. Aguirre-Chen, T. Kietzmann, I. Saul, R. Busto, M.D. Ginsberg, Nuclear localization of the hypoxia-regulated pro-apoptotic protein BNIP3 after global brain ischemia in the rat hippocampus, *Brain Res.* 1001 (2004) 133–142.
- [14] G. Chen, R. Ray, D. Dubik, L. Shi, J. Cizeau, R.C. Bleackley, S. Saxena, R.D. Gietz, A.H. Greenberg, The E1B 19K/Bcl-2-binding protein Nip3 is a dimeric mitochondrial protein that activates apoptosis, *J. Exp. Med.* 186 (1997) 1975–1983.
- [15] W.G. Mayhan, VEGF increases permeability of the blood–brain barrier via a nitric oxide synthase/cGMP-dependent pathway, *Am. J. Physiol.* 276 (1999) C1148–C1153.
- [16] R.P. Ostrowski, A.R. Colohan, J.H. Zhang, Molecular mechanisms of early brain injury after subarachnoid hemorrhage, *Neurol. Res.* 28 (2006) 399–414.
- [17] J.H. Garcia, S. Wagner, K.F. Liu, X.J. Hu, Neurological deficit and extent of neuronal necrosis attributable to middle cerebral artery occlusion in rats. Statistical validation, *Stroke* 26 (1995) 627–634. discussion 635.
- [18] T. Sugawara, R. Ayer, V. Jadhav, J.H. Zhang, A new grading system evaluating bleeding scale in filament perforation subarachnoid hemorrhage rat model, *J. Neurosci. Methods* 167 (2008) 327–334.
- [19] D. Yin, C. Zhou, I. Kusaka, J.W. Calvert, A.D. Parent, A. Nanda, J.H. Zhang, Inhibition of apoptosis by hyperbaric oxygen in a rat focal cerebral ischemic model, *J. Cereb. Blood Flow Metab.* 23 (2003) 855–864.
- [20] C. Zhou, Y. Li, A. Nanda, J.H. Zhang, HBO suppresses Nogo-A, Ng-R, or RhoA expression in the cerebral cortex after global ischemia, *Biochem. Biophys. Res. Commun.* 309 (2003) 368–376.
- [21] Y. Sun, C. Zhou, P. Polk, A. Nanda, J.H. Zhang, Mechanisms of erythropoietin-induced brain protection in neonatal hypoxia-ischemia rat model, *J. Cereb. Blood Flow Metab.* 24 (2004) 259–270.
- [22] R. Yu, L. Gao, S. Jiang, P. Guan, B. Mao, Association of HIF-1 α expression and cell apoptosis after traumatic brain injury in the rat, *Chin. J. Traumatol.* 4 (2001) 218–221.
- [23] J.C. Chavez, J.C. LaManna, Activation of hypoxia-inducible factor-1 in the rat cerebral cortex after transient global ischemia: potential role of insulin-like growth factor-1, *J. Neurosci.* 22 (2002) 8922–8931.
- [24] K.L. Jin, X.O. Mao, T. Nagayama, P.C. Goldsmith, D.A. Greenberg, Induction of vascular endothelial growth factor and hypoxia-inducible factor-1 α by global ischemia in rat brain, *Neuroscience* 99 (2000) 577–585.
- [25] Y. Jiang, J. Wu, R.F. Keep, Y. Hua, J.T. Hoff, G. Xi, Hypoxia-inducible factor-1 α accumulation in the brain after experimental intracerebral hemorrhage, *J. Cereb. Blood Flow Metab.* 22 (2002) 689–696.
- [26] J. Yan, B. Zhou, S. Taheri, H. Shi, Differential effects of HIF-1 inhibition by YC-1 on the overall outcome and blood–brain barrier damage in a rat model of ischemic stroke, *PLoS One* 6 (2011) e27798.
- [27] C. Chen, Q. Hu, J. Yan, X. Yang, X. Shi, J. Lei, L. Chen, H. Huang, J. Han, J.H. Zhang, C. Zhou, Early inhibition of HIF-1 α with small interfering RNA reduces ischemic-reperfused brain injury in rats, *Neurobiol. Dis.* 33 (2009) 509–517.
- [28] W. Chen, V. Jadhav, J. Tang, J.H. Zhang, HIF-1 α inhibition ameliorates neonatal brain injury in a rat pup hypoxic-ischemic model, *Neurobiol. Dis.* 31 (2008) 433–441.
- [29] L. Li, Y. Qu, J. Li, Y. Xiong, M. Mao, D. Mu, Relationship between HIF-1 α expression and neuronal apoptosis in neonatal rats with hypoxia-ischemia brain injury, *Brain Res.* 1180 (2007) 133–139.
- [30] P. Marchetti, M. Castedo, S.A. Susin, N. Zamzami, T. Hirsch, A. Macho, A. Haeflner, F. Hirsch, M. Geuskens, G. Kroemer, Mitochondrial permeability transition is a central coordinating event of apoptosis, *J. Exp. Med.* 184 (1996) 1155–1160.
- [31] N. Zamzami, S.A. Susin, P. Marchetti, T. Hirsch, I. Gomez-Monterrey, M. Castedo, G. Kroemer, Mitochondrial control of nuclear apoptosis, *J. Exp. Med.* 183 (1996) 1533–1544.
- [32] R. Ray, G. Chen, C. Vande Velde, J. Cizeau, J.H. Park, J.C. Reed, R.D. Gietz, A.H. Greenberg, BNIP3 heterodimerizes with Bcl-2/Bcl-X(L) and induces cell death independent of a Bcl-2 homology 3 (BH3) domain at both mitochondrial and nonmitochondrial sites, *J. Biol. Chem.* 275 (2000) 1439–1448.
- [33] C. Vande Velde, J. Cizeau, D. Dubik, J. Alimonti, T. Brown, S. Israels, R. Hakem, A.H. Greenberg, BNIP3 and genetic control of necrosis-like cell death through the mitochondrial permeability transition pore, *Mol. Cell. Biol.* 20 (2000) 5454–5468.
- [34] R.K. Bruick, Expression of the gene encoding the proapoptotic Nip3 protein is induced by hypoxia, *Proc. Natl. Acad. Sci. USA* 97 (2000) 9082–9087.
- [35] C. Chen, Q. Hu, J. Yan, J. Lei, L. Qin, X. Shi, L. Luan, L. Yang, K. Wang, J. Han, A. Nanda, C. Zhou, Multiple effects of 2ME2 and D609 on the cortical expression of HIF-1 α and apoptotic genes in a middle cerebral artery occlusion-induced focal ischemia rat model, *J. Neurochem.* 102 (2007) 1831–1841.
- [36] J. Althaus, M. Bernaudin, E. Petit, J. Toutain, O. Touzani, A. Rami, Expression of the gene encoding the pro-apoptotic BNIP3 protein and stimulation of hypoxia-inducible factor-1 α (HIF-1 α) protein following focal cerebral ischemia in rats, *Neurochem. Int.* 48 (2006) 687–695.
- [37] J. Claassen, J.R. Carhuapoma, K.T. Kreiter, E.Y. Du, E.S. Connolly, S.A. Mayer, Global cerebral edema after subarachnoid hemorrhage: frequency, predictors, and impact on outcome, *Stroke* 33 (2002) 1225–1232.
- [38] J. Josko, B. Gwozdz, S. Hendryk, H. Jedrzejowska-Szypulka, J. Slowinski, J. Jochem, Expression of vascular endothelial growth factor (VEGF) in rat brain after subarachnoid haemorrhage and endothelin receptor blockage with BQ-123, *Folia Neuropathol.* 39 (2001) 243–251.
- [39] Z.G. Zhang, L. Zhang, Q. Jiang, R. Zhang, K. Davies, C. Powers, N. Bruggen, M. Chopp, VEGF enhances angiogenesis and promotes blood–brain barrier leakage in the ischemic brain, *J. Clin. Invest.* 106 (2000) 829–838.
- [40] N. van Bruggen, H. Thibodeaux, J.T. Palmer, W.P. Lee, L. Fu, B. Cairns, D. Tumas, R. Gerlai, S.P. Williams, M. van Lookeren Campagne, N. Ferrara, VEGF antagonism reduces edema formation and tissue damage after ischemia/reperfusion injury in the mouse brain, *J. Clin. Invest.* 104 (1999) 1613–1620.